Sakarya University Journal of Science

ISSN : 2147-835X
Publisher : Sakarya University

Vol. 28, No. 2, 237-248, 2024
DOI: https://doi.org/10.16984/saufenbilder.1199910

Research Article

The Oxidase Mimicking Activity of MnOx NPs/Co_3O_4 NPs Hybrid Nanozyme for Glucose Oxidation

Bekir Çakıroğlu

Sakarya University, Biomedical, Magnetic and Semiconductor Materials Research Center (BIMAS-RC), Sakarya, Türkiye, bekircakiroglu@sakarya.edu.tr

ARTICLE INFO

Keywords:
Nanozyme
Co_3O_4 NPs
MnOx NPs
Colorimetric Assay
Sustainability

Article History:
Received: 05.10.2022
Accepted: 08.01.2024
Online Available: 22.04.2024

ABSTRACT

Herein, the hybrid nanozyme MnO_x NPs/Co_3O_4 NPs on indium tin oxide coated glass substrate (ITO) was manufactured by imparting the porous morphology with its distinct merits: its surface valence states, oxygen vacancies, large surface area, and abundant active sites. The oxidase-like activity was investigated via the catalytic oxidation of chromogenic substrate in the presence of glucose visualized by the eyes. MnO_x NPs containing Mn^{2+} and Mn^{3+} have a superior ability to oxidize glucose by reducing dissolved oxygen and producing H_2O_2. Co_3O_4 NPs, in turn, reduce H_2O_2 with concomitant 3,3′,5,5′-tetramethylbenzidine (TMB) oxidization. Thus, the nanozyme mimics the dual roles of glucose oxidase and peroxidase. The oxidase-like activity of hybrid nanozyme for glucose was found to be higher than those of single components. The nanozyme responded to glucose with a linear range from 60 µM to 1200 µM. The acceptable performance is probably due to the facilitated access of glucose to the proximity of the sensor surface. Good reproducibility was accomplished by virtue of the meticulous construction of NPs. Without functionalization and enzyme utilization, the fabricated nanozyme holds promise as a substitute for peroxidase and oxidase for detecting glucose.

1. Introduction

Natural enzymes have been widely used due to their effective and specific catalytic activity on substrates under mild conditions [1–4]. However, enzymes face inherent drawbacks, such as high-cost purification and low storage and operational stability [5–6]. Additionally, they are susceptible to pH, temperature, ionic strength, surfactants, and organic solvents, and digestion by proteases hampers their widespread use [7]. Since the exciting breakthrough of Fe_3O_4 MNPs exhibiting peroxidase-like activity in 2007 [8], considerable efforts have been devoted to exploring efficient artificial enzymes with intrinsic enzyme-like activities, aka "nanozymes", to address these difficulties [9].

Nanozymes have been at the forefront as a viable alternative to facilitate analyte sensing owing to their striking merits [10]. These include adjustable catalytic activity, high stability against harsh environments, facile surface modification, and low-cost and straightforward production [11–12]. However, nanozymes could not selectively catalyze one specific substrate like enzymes [13]. Improving the asymmetric selectivity of nanozymes is one of the potential challenges [14].

Hitherto, the enzymatic activity and selectivity of nanozymes have been tailored by surface modification [15], particle size adjustment [16], heterogeneous atomic doping [17], and morphology [18]. The large surface area exposes more active sites, and preferential exposure of catalytically active atoms increases the activity [19]. Surface defects such as ledges, adatoms, vacancies and kinks are coordinatively

Cite as: B. Çakıroğlu (2024). The Oxidase Mimicking Activity of MnOx NPs/Co3O4 NPs Hybrid Nanozyme for Glucose Oxidation, *Sakarya University Journal of Science,* 28(2), 237-248. https://doi.org/10.16984/saufenbilder.1199910

unsaturated reactive sites and strongly adsorb substrates [20].

Encouragingly, the catalytic performance of nanozymes has been synergically improved by functionally assembling several nanozymes showing the same enzyme-mimicking activity [21].

Up to now, most of the reported nanozymes have mirrored peroxidase-like activity; thus, the oxidase-like nanozymes are becoming more attractive [12, 22–23]. Noble metal nanoparticles such as Au NPs and their alloys have exhibited GOx-like activity owing to their remarkable oxygen reduction catalytic activities [12]. However, high-cost production hinders widespread applications. Multivalent manganese(II,III) oxide (MnO_x) was reported to possess intrinsic oxidase-like activity due to its multiple oxidation states, along with satisfying features such as low-cost production, remarkable catalytic activity, non-toxicity, and environmental friendliness [24–26]. Likewise, cobalt(II, III) oxide (Co_3O_4) nanomaterials have rich redox properties depending on their morphology and multiple catalytic activities, closely correlated to medium pH. Also, Co_3O_4 nanozymes catalyze H_2O_2 by showing peroxidase-like activity [17–18].

Conventional glucose detection has been performed by combining the corresponding oxidase enzyme and peroxidase nanozyme [27]. However, the different reaction conditions render the operation intricate. Thus, one-step colorimetric glucose-sensing will impel the development of nanozyme-based sensors [28–30].

In this article, a nano-structured hybrid nanozyme was reported for glucose oxidation. Its oxidase mimics activity was investigated in the presence of a chromogenic substrate.

2. Materials and Methods

2.1. Reagents and chemicals

ITO glass slides, ethanol (anhydrous, ≥99.8%), manganese(II) chloride tetrahydrate ($MnCl_2.4H_2O$)**,** Cobalt(II) chloride hexahydrate and D-(+)-glucose monohydrate were obtained from Merck. TMB, sodium hydroxide (NaOH), isopropyl alcohol, potassium iodide (KI), ethylenediaminetetraacetic acid (EDTA), iron(II) sulfate heptahydrate, sucrose, lactose, and maltose were purchased from Sigma-Aldrich. Acetate buffer solution (ABS) was prepared using glacial acetic acid (Merck) and sodium acetate (Sigma-Aldrich). Hydrochloric acid-potassium chloride buffer (0.1 M, pH 2.0) was prepared using potassium chloride (Sigma-Aldrich) and hydrochloric acid (Merck). All chemicals were used as received, and deionized water (DW) was obtained from a Labconco Water Pro BT purification system.

2.2. Preparation of Co_3O_4 NPs

The ITO electrodes (50 mm length × 10 mm width × 1.1 mm thickness; surface resistivity 8-12 Ω/sq) were consecutively pre-cleaned by sonication in acetone, 1 M NaOH, ethanol/DW mixture (1:1, v/v), and DW for 15 min, before being dried in a vacuum oven.
Co_3O_4 NPs were manufactured as follows. 0.1 M $CoCl_2$ in isopropanol was applied on the glass surfaces, and the substrates were kept in the oven at 75 °C for 24 h and calcined at 450 °C for 12 h in a muffle furnace to crystallize the samples. The resulting product is designated as Co_3O_4 NPs/ITO.

2.3. Preparation of MnO_x NPs on Co_3O_4 NPs

The successful ionic layer adsorption and reaction (SILAR) was used to attain MnO_x deposition. The free-standing substrates were dipped into the cationic precursor of 0.3 M $MnCl_2$ (pH: 1) for 20 s to deposit Mn^{2+} on the substrate. The substrate was then rinsed with DW and then soaked in an anionic precursor of 0.01 M NaOH (pH: 13) for 20 s, where OH^- ions react with Mn^{2+} to obtain a manganese oxide layer followed by rinsing with DW to eliminate loosely bound species. This cycle was repeated 5, 10, and 15 times for structural optimization, and the product (MnO_x NPs/Co_3O_4 NPs/ITO) was dried at 60 ^oC in an oven.

2.4. Oxidase-like activity measurements

For the detection of glucose, 2.5 mL of 0.4 mM TMB aliquots was prepared in 200 mM ABS pH 3.8 with free-standing nanozyme substrate, and 50 µL of varying glucose concentrations (0-1600 µM) were added into the above mixture and incubated for 8 min at 35 ºC in cuvettes. Then, the free-standing substrate (MnO_x NPs/Co_3O_4 NPs/ITO) was removed from the reaction medium, and the absorbance measurements were carried out at 652 nm. Each experiment was repeated at least four times.

2.5. Characterization

The morphological features of nanozyme components were characterized by field emission scanning electron microscopy (FESEM) recorded on a FEI Quanta FEG 450. The crystalline planes were elucidated by X-ray diffraction (XRD, RIGAKU D/Max 2200), using monochromatized Cu radiation resource (λ= 1.5045 Å). UV visible (UV-Vis) absorbance and diffuse reflectance spectroscopy (DRS, $BaSO_4$ as reference) spectra were recorded using a Shimadzu UV-2600 spectrophotometer at 200-800 nm.

3. Results and Discussions

3.1. Characterization of free-standing nanozyme substrate

An outstanding nanozyme for glucose detection was fabricated, as illustrated in Figure 1. The solution-based nanozymes have an unwanted effect on the absorption spectrum, whereas the free-standing nanozymes can negate this interference by removing it from the post-reaction medium. The nanozyme preserved the multi-enzyme-mimicking activity in months of usage without additional storage conditions. The top-view TEM image of Co_3O_4 NPs displayed flakes of nanoparticle aggregates. The size of the Co_3O_4 NPs estimated from the image is 23 nm (Figure 2A). After MnO_x NPs' deposition, the morphological alteration is evident that MnO_x NPs are deposited on Co_3O_4 NPs (Figure 2B). The size of the deposited MnO_x NPs was calculated to be around 25 nm nearly the same size as Co_3O_4 NPs. The NP-coated substrates exhibited opalescence under the light (Figure 2B inset).

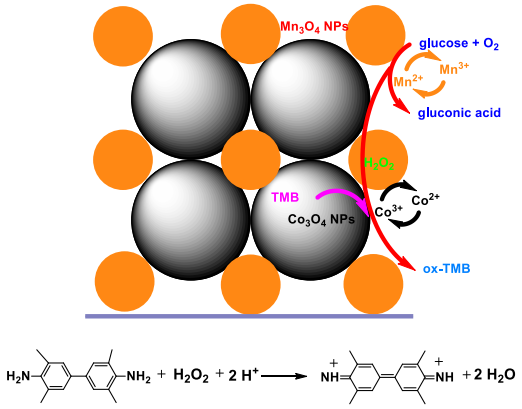

Figure 1. The one-pot nonenzymatic colorimetric glucose detection using the free-standing nanozyme hybrid

Figure 2C shows the XRD pattern of the hybrid nanozyme. The peaks located at 2θ = 19.0°, 31.3°, 36.8°, 38.5°, 44.8°, 55.6°, 59.3°, and 65.2°, respectively, correspond to the (111), (220), (311), (222), (400), (422), (511), and (440) planes of face-centered cubic (fcc) spinel Co_3O_4 (JCPDS No. 74-2120) [31]. The prominent diffraction peaks of MnO NPs appearing at 35.12°, 41.26°, 59.16°, and 71.42° indexed to (111), (200), (220), and (311) crystalline planes of MnO spheres (JCPDS no. 07-0230) implying that MnO was formed on Co_3O_4 NPs. The peak at 32.75° corresponds to the main peak of Mn_2O_3 NPs (222) (JCPDS no. 71-0636), which can efficiently oxidase TMB [32]. Additional diffraction peaks could be associated with the indium tin oxide layer on the glass.

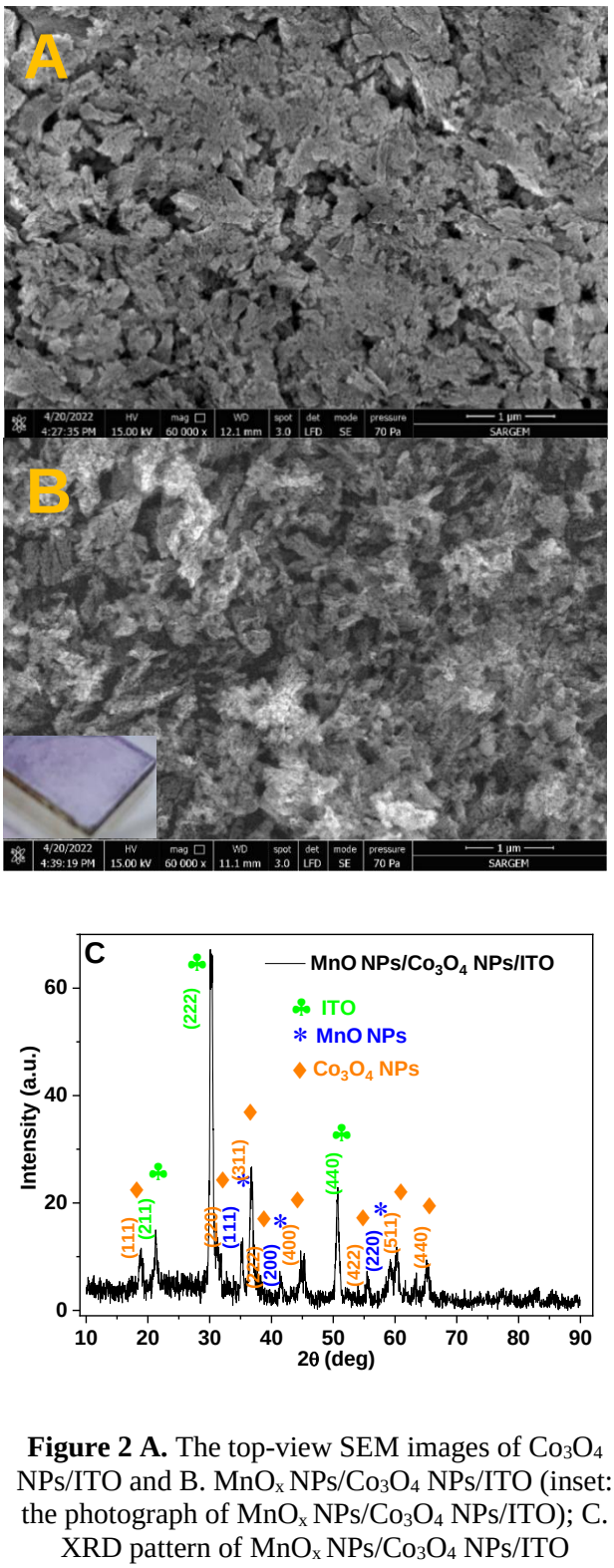

Figure 2 A. The top-view SEM images of Co_3O_4 NPs/ITO and B. MnO_x NPs/Co_3O_4 NPs/ITO (inset: the photograph of MnO_x NPs/Co_3O_4 NPs/ITO); C. XRD pattern of MnO_x NPs/Co_3O_4 NPs/ITO

Figure 3A exhibits the reflection spectra of NP-coated substrates. NPs display intense and typical reflection bands due to their photonic properties. After the MnO_x deposition, the reflection band was blue-shifted owing to the narrowing pore size of NPs. UV-Vis spectrum revealed the absorbance band of the nanozyme in the visible region (Figure 3B).

3.2. Mechanism of peroxidase- and oxidase-like activities of the hybrid nanozyme

The time-dependent absorbance intensity of TMB reaches the maximum after 8 min of incubation, suggesting that the redox process between TMB and nanozyme is a surface-mediated reaction. The medium pH effect was screened in 200 mM ABS at various pH values ranging from 2 to 5.8. Owing to the similar structure of TMB with a diamine, basic pH brings about poor solubility of TMB. The hybrid nanozyme activity demonstrated a volcano-shaped dependence on pH with the optimal point of pH 3.8 and is stable over a broad temperature range from 15 °C to 40 °C with an optimal value of 35 °C.

A significant absorbance was observed at the maximum wavelength (652 nm) for Co_3O_4 NPs/ITO in the presence of 5 mM glucose in 200 mM in ABS pH 3.8 at optimal temperature, confirming the oxidase and peroxidase-like activity of NPs (Figure 3C). Also, the hybrid nanozyme exhibited boosted absorbance at 652 nm relative to Co_3O_4 NPs/ITO, implying that both Co_3O_4 NPs and MnO_x NPs were inevitable to enhance the intrinsic oxidase-like activity. According to the absorbance spectra, the optimal SILAR cycle for MnO_x NP deposition was ten cycles (Figure 3C).

The absorbance spectra were measured in the presence of various scavengers and activators to understand the mechanism of hybrid nanozyme (Figure 3D). The glucose oxidase-like activity was enormously inhibited upon adding catalase and Fe(II) EDTA, ascertaining the generation of H_2O_2 [33].

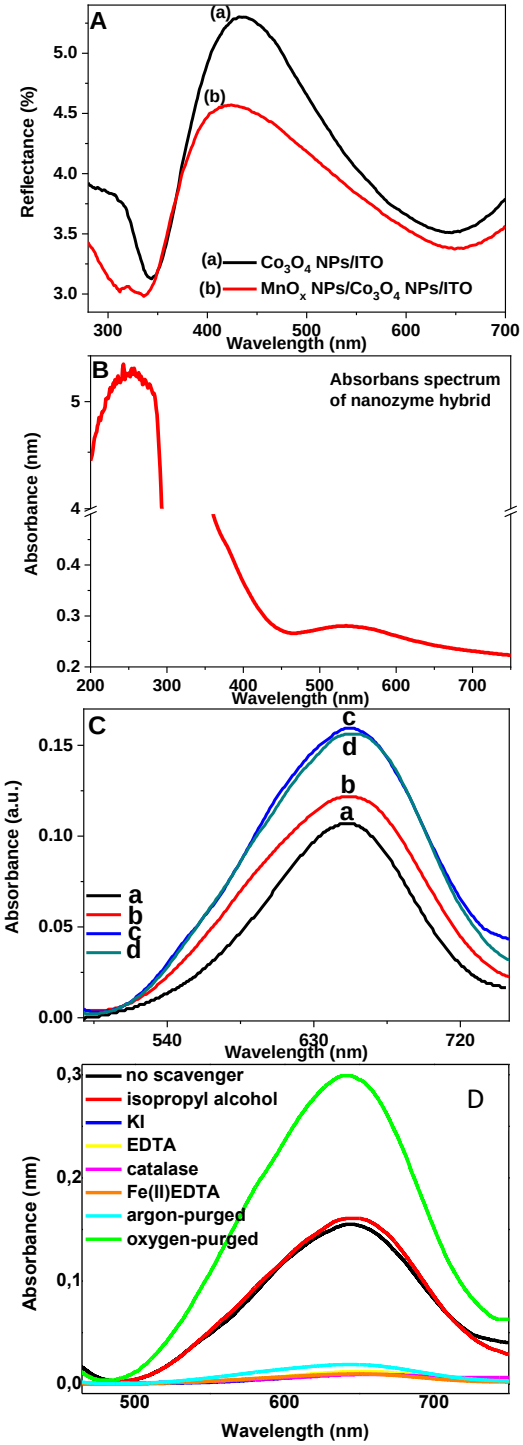

Figure 3 A. Reflectance spectra of materials; B. UV–visible absorbance spectra of nanozyme; C. UV–visible absorbance spectra of ox-TMB generated by the different nanozymes: (a) Co_3O_4 NPs/ITO, (b,c,d) 5, 10, 15 cycles MnO_x NPs/Co_3O_4 NPs/ITO, respectively, D. Scavengers and activator effect on multiple enzyme-like activities

To determine whether H_2O_2 is reduced to hydroxyl radicals, IPA, a hydroxyl radical scavenger, was added, and no absorbance diminishing was observed. Ergo, H_2O_2 is probably reduced to water[34]. The mechanism was further validated using KI and EDTA, the most used hole scavengers, and the oxidation of TMB was fully inhibited [35]. Therefore, the electron vacancies play a pivotal role, and in the oxidase-mimicking activity, the hybrid nanozyme will accept electrons by oxidizing the chromogenic substrate [36].

The effect of oxygen on oxidation was surveyed to reveal the oxidase-mimicking activity. The ox-TMB absorption intensity was reduced to almost zero in the argon-saturated solution, confirming that oxygen takes part in the reaction. In the presence of O_2, a substantial increase in absorbance was observed, implying oxygen consumption during catalysis. In line with these findings, the multi-enzyme mimic activities of the hybrid nanozyme were elucidated tentatively, as illustrated in Figure 1. The initial adsorptions of oxygen and TMB are the principal contributing factors to the dual enzyme activity.

The oxygen vacancies of MnO_x NPs were beneficial for oxygen adsorption to generate active electrophilic oxygen species [37]. Thus, MnO_x NPs serve as a GOx-like nanozyme that oxidizes glucose with the concomitant reduction of O_2 to H_2O_2 (eq. 1). Also, (111) plane of spinel Co_3O_4 is the most active facet for the oxygen reduction activities owing to the density of highly exposed Co^{2+} active sites in the plane [38]. Therefore, Co_3O_4 NPs can reduce oxygen along with MnO_x. Simultaneously, Co (III) in Co_3O_4 NPs obtains electrons from TMB and then converts to Co (II), thus oxidizing TMB. The catalysts with lower redox potential, such as Co_3O_4, are thermodynamically favorable to transfer electrons to H_2O_2 [34]. Therefore, Co (II) can transfer electrons to in situ generated H_2O_2 and then convert back to Co (III) (eq. 2), mimicking HRP.

$$O_2+2H^++2e^-\rightarrow H_2O_2 \quad (1)$$

$$H_2O_2+2H^++2e^-(Co\ (II))\rightarrow 2H_2O(Co\ (III)) \quad (2)$$

The oxidase-mimicking activity could be attributed to several factors. The NPs with internal voids provide large surface areas and copious catalytically active sites [39]. The accessible surface for the substrate could facilitate concurrent tandem catalysis in NPs [40]. Furthermore, the adsorbent behavior of

nanozyme brings the target molecule of interest close to the nanozyme, which makes the cascade reactions infinitely near each other by preventing the mass transfer process of reactants and intermediates [41]. The remarkable electron transfer occurring on the specific facet is conducive to the escalated nanozyme activity [19].

3.3. Colorimetric glucose detection with free-standing nanozyme and steady-state kinetic assay

The nanozyme exhibited a linear dependence for glucose concentrations ranging from 60 µM to 1200 µM (y=0.000127x + 0.00342, R^2 = 0.9969), implying that detection is likely viable (Figure 4A, B, C). The color of oxidized TMB was visible to the naked eye at glucose concentrations lower than 0.2 mM (Fig. 4A inset). The comparison of the prepared nanozyme with the ones reported in the literature is listed in Table 1.

According to Table 1, a wider measurement range with a lesser operation time was concluded. The large surface area of nanozyme was thought to push the dynamic range to the mM levels. According to the literature, nanozymes with glucose oxidase-like activity are mostly gold-based expensive materials. Herein, a cost-effective nanozyme material containing two metal oxides was proposed. The limit of detection (LOD) was estimated based on 3(standard deviation of 20 blank measurements/ slope of the linear fit) and was determined as 18 µM. The limit of quantification was estimated based on 10(standard deviation of 20 blank measurements/ slope of the linear fit) and was calculated as 60 µM.

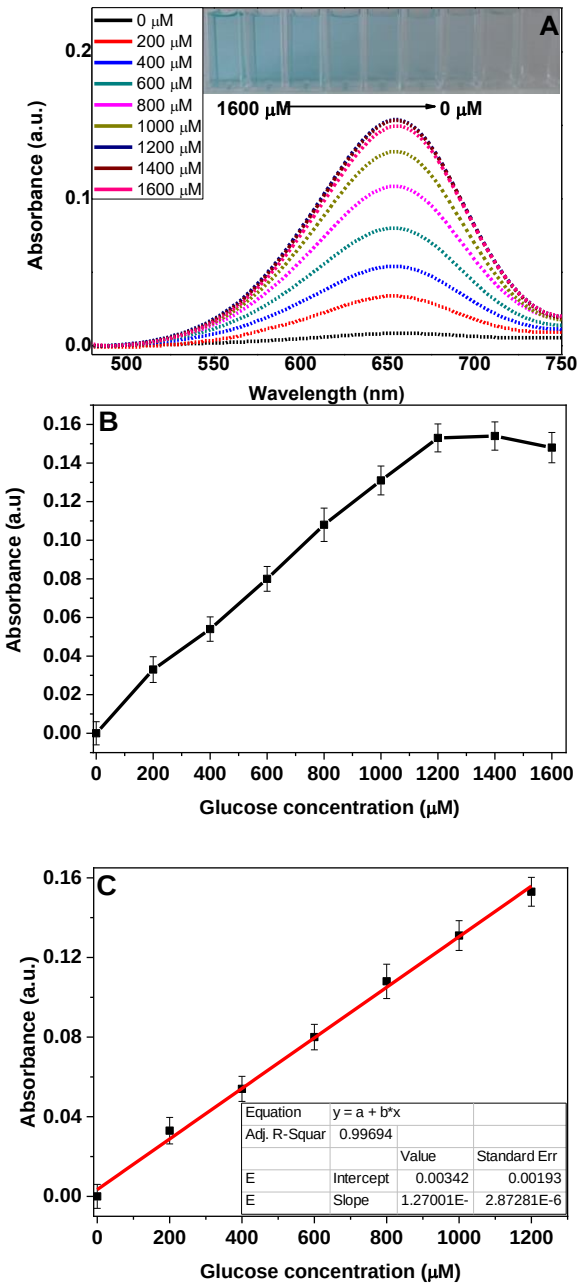

Figure 4 A. The absorbance spectra vs. glucose concentration (inset shows the corresponding post-reaction colorizations in various glucose concentrations); B. The absorbance vs. glucose concentration plot and C. the calibration curve for glucose detection

Typical Michaelis-Menten curves were obtained for glucose oxidation, and kinetic parameters such as the Michaelis-Menten constant (*K*m) were obtained using the following equation [42]:

$$1/Vo = Km/Vmax + (1/[S])(1/Km) \quad (3)$$

A lower *K*m value is desirable because Km represents the substrate's affinity. Km values were found to be 0.6 mM, lower than native GOx

(4.1 mM) [42], indicating a high affinity for glucose.

3.4. The nanozyme sensor performance

Also, the fabrication process was found to be effective for reproducible sensor production, and the satisfying feasibility was confirmed, outlining the robustness of the nanozyme (Figure 5). The sensor stability was studied for four weeks, and negligible loss in the catalytic activity of less than 3% was found (Figure 6).

The selectivity was assessed by exposing the sensor to 1.2 mM glucose and 1.2 mM glucose analogs, viz. lactose, sucrose, and maltose. The response was not remarkably influenced in the presence of maltose. The absorbance increased to some extent in the presence of lactose and sucrose due to the oxidation of analogs (Figure 7). The plausible reason for this finding is that the nanozyme can lead to the hydrolysis of disaccharides. Some disaccharides may undergo efficient hydrolysis, thus releasing more glucose.

Table 1. The performance comparison of the reported nanozyme-based glucose sensors

Material	Method/ temperature	LOD (μM)	Linear range (mM)	Duration (min)	Ref.
MnO_x NPs/Co_3O_4 NPs/ITO	spectrophotometric detection/ 35 ºC	18	0.06–1.2	8	Current study
ITO/PbS/SiO_2/AuNPs	photoelectrochemical detection/ room temp.	0.46	0.001–1.0	-	[43]
CS-GO[1]	spectrophotometric detection/ room temp.	0.5	2.5–5.0	10	[44]
m-GCN[2]	spectrophotometric detection/ 25 °C	0.8	0.01–1000	0.5	[45]
m-GCN-chitin-acetic acid	spectrophotometric detection/ 30 ºC	0.055	0.005–1	3	[29]
MnO_2 nanoflakes	spectrophotometric detection/ 37 °C	1	0.005–1.2	15	[46]
Au@BSA NPs-GO	spectrophotometric detection/ n.a.[3]	0.6	0.001–0.3	30	[47]
Au NP@Au NCs	spectrophotometric detection/ room temp.	20	0.05-0.4	40	[48]

[1] chitosan-functionalized graphene oxide
[2] modified graphitic carbon nitride
[3]not available

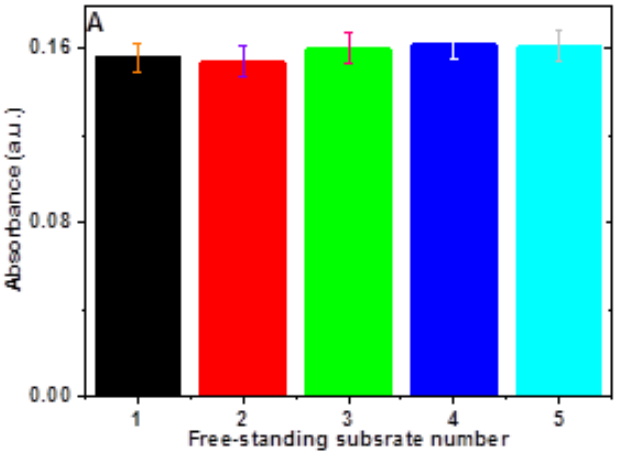

Figure 5. The reproducibility of the sensor

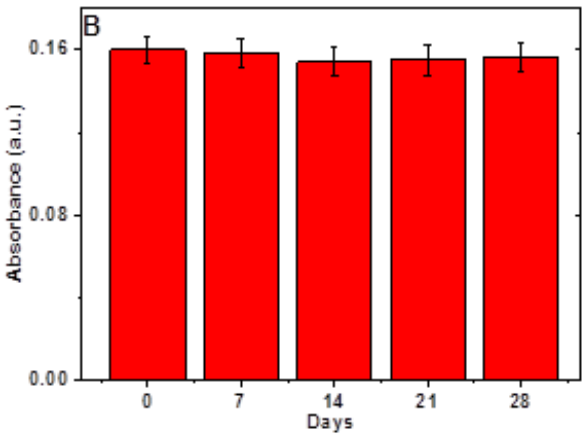

Figure 6. The stability study of the sensor

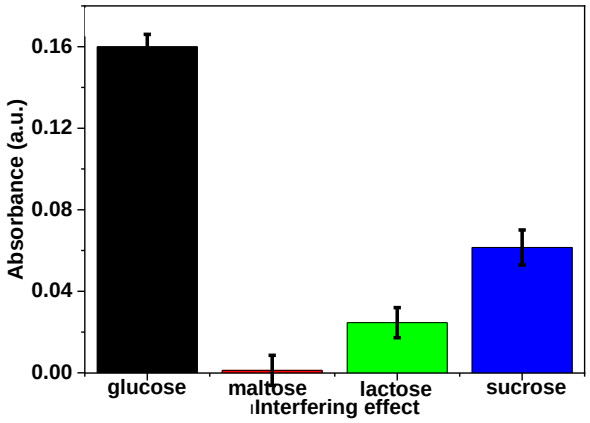

Figure 7. The selectivity of the free-standing nanozyme for glucose detection when exposed to glucose and glucose analogs

4. Conclusion

In summary, MnO_x NPs/Co_3O_4 NPs/ITO was synthesized with favorable morphology for reactants and products, which could catalyze glucose oxidation by molecular oxygen to produce H_2O_2. The coupled oxidase and peroxidase-mimicking activity of MnO_x NPs/Co_3O_4 NPs/ITO was utilized for colorimetric glucose sensing. Since Co_3O_4 NPs and MnO_x NPs are mainly peroxidase-like and oxidase-like mimics, respectively, the assembly of these nanozymes exhibited specific and remarkable glucose sensing performance. The rational design of NPs grants access to abundant catalytically active sites and enhances the catalytic activity. This work may find its unique niche as an efficient biomimetic oxidase for glucose monitoring in the sensor area.

Article Information Form

Acknowledgments
The author would like to thank Prof. Dr. Mehmet Nebioğlu and Assoc. Prof. Dr. Emrah Bulut for their valuable contributions.

Funding
The author has not received any financial support for the research, authorship or publication of this study.

The Declaration of Ethics Committee Approval
This study does not require ethics committee permission or any special permission.

The Declaration of Research and Publication Ethics
The author of the paper declare that he complies with the scientific, ethical and quotation rules of SAUJS in all processes of the paper and that he does not make any falsification on the data collected. In addition, he declares that Sakarya University Journal of Science and its editorial board have no responsibility for any ethical violations that may be encountered, and that this study has not been evaluated in any academic publication environment other than Sakarya University Journal of Science.

References

[1] E. Vargas, H. Teymourian, F. Tehrani, E. Eksin, E. Sánchez-Tirado, P. Warren, A. Erdem, E. Dassau, J. Wang, “Enzymatic/Immunoassay Dual-Biomarker Sensing Chip: Towards Decentralized Insulin/Glucose Detection,” Angewandte Chemie International Edition, vol. 58, no. 19, pp. 6376–6379, 2019.

[2] A. J. Gross, M. Holzinger, S. Cosnier, “Buckypaper bioelectrodes: Emerging materials for implantable and wearable biofuel cells,” Energy & Environmental Science journal, vol. 11, no. 7, pp. 1670–1687, 2018.

[3] M. Holzinger, P. H. M. Buzzetti, S. Cosnier, “Polymers and nano-objects, a rational combination for developing health monitoring biosensors,” Sensors and Actuators B: Chemical, vol. 348, p. 130700, 2021.

[4] B. Çakıroğlu, J. Chauvin, A. Le Goff, K. Gorgy, M. Özacar, M. Holzinger, “Photoelectrochemically-assisted biofuel cell constructed by redox complex and g-C3N4 coated MWCNT bioanode,” Biosensors and Bioelectronics, vol. 169, p. 112601, Dec. 2020.

[5] W. Guan, X. Duan, M. A. Reed, "Highly specific and sensitive non-enzymatic determination of uric acid in serum and urine by extended gate field effect transistor sensors," Biosensors and Bioelectronics, vol. 51, pp. 225–231, 2014.

[6] S. Chaiyo, E. Mehmeti, W. Siangproh, T. L. Hoang, H. P. Nguyen, O. Chailapakul, K. Kalcher, "Non-enzymatic electrochemical detection of glucose with a disposable paper-based sensor using a cobalt phthalocyanine–ionic liquid–graphene composite," Biosensors and Bioelectronics, vol. 102, pp. 113–120, 2018.

[7] A. L. Rinaldi, R. Carballo, "Impedimetric non-enzymatic glucose sensor based on nickel hydroxide thin film onto gold electrode," Sensors and Actuators B: Chemical, vol. 228, pp. 43–52, 2016.

[8] L. Gao, J. Zhuang, L. Nie, J. Zhang, Y. Zhang, N. Gu, T. Wang, J. Feng, D. Yang, S. Perrett, X. Yan, "Intrinsic peroxidase-like activity of ferromagnetic nanoparticles," Nature Nanotechnology, vol. 2, no. 9, pp. 577–583, 2007.

[9] D. Jiang, D. Ni, Z. T. Rosenkrans, P. Huang, X. Yan, W. Cai, "Nanozyme: new horizons for responsive biomedical applications," Chemical Society Reviews, vol. 48, no. 14, pp. 3683–3704, 2019.

[10] D. Duan, K. Fan, D. Zhang, S. Tan, M. Liang, Y. Liu, J. Zhang, P. Zhang, Wei Liu, X. Qiu, G. P. Kobinger, G. F. Gao, X. Yan, "Nanozyme-strip for rapid local diagnosis of Ebola," Biosensors and Bioelectronics, vol. 74, pp. 134–141, 2015.

[11] M. N. Karim, S. R. Anderson, S. Singh, R. Ramanathan, V. Bansal, "Nanostructured silver fabric as a free-standing NanoZyme for colorimetric detection of glucose in urine," Biosensors and Bioelectronics, vol. 110, pp. 8–15, 2018.

[12] H. Zhang, X. Liang, L. Han, F. Li, "'Non-Naked' Gold with Glucose Oxidase-Like Activity: A Nanozyme for Tandem Catalysis," Small, vol. 14, no. 44, p. 1803256, 2018.

[13] Y. Park, P. K. Gupta, V.-K. Tran, S. E. Son, W. Hur, H. B. Lee, J. Y. Park, S. N. Kim, G. H. Seong, "PVP-stabilized PtRu nanozymes with peroxidase-like activity and its application for colorimetric and fluorometric glucose detection," Colloids Surfaces B Biointerfaces, vol. 204, p. 111783, 2021.

[14] Q. Wang, S. Liu, Z. Tang, "Recent progress in the design of analytical methods based on nanozymes," Journal of Materials Chemistry B, vol. 9, no. 39, pp. 8174–8184, 2021.

[15] B. Gökçal, Ç. Kip, A. Tuncel, "One-pot, direct glucose detection in human whole blood without using a dilution factor by a magnetic nanozyme with dual enzymatic activity," Journal of Alloys and Compounds, vol. 843, p. 156012, 2020.

[16] Q. Chen, S. Li, Y. Liu, X. Zhang, Y. Tang, H. Chai, Y. Huang, "Size-controllable Fe-N/C single-atom nanozyme with exceptional oxidase-like activity for sensitive detection of alkaline phosphatase," Sensors and Actuators B: Chemical, vol. 305, p. 127511, 2020.

[17] Q. Chen, X. Zhang, S. Li, J. Tan, C. Xu, Y. Huang, "MOF-derived Co3O4@Co-Fe oxide double-shelled nanocages as multi-functional specific peroxidase-like nanozyme catalysts for chemo/biosensing and dye degradation," Chemical Engineering Journal, vol. 395, no. March, p. 125130, 2020.

[18] X. Zhang, Y. Lu, Q. Chen, Y. Huang, "A tunable bifunctional hollow Co3O4/MO3 (M = Mo, W) mixed-metal oxide nanozyme for sensing H2O2 and screening acetylcholinesterase activity and its inhibitor," Journal of Materials Chemistry B, vol. 8, no. 30, pp. 6459–6468, 2020.

[19] W. Wu, L. Huang, E. Wang, S. Dong, "Atomic engineering of single-atom nanozymes for enzyme-like catalysis," Chemical Science, vol. 11, no. 36, pp. 9741–9756, 2020.

[20] J. Zhang, Q. Kuang, Y. Jiang, Z. Xie, "Engineering high-energy surfaces of noble metal nanocrystals with enhanced catalytic performances," Nano Today, vol. 11, no. 5, pp. 661–677, 2016.

[21] P. Gallay, M. Eguílaz, G. Rivas, "Designing electrochemical interfaces based on nanohybrids of avidin functionalized-carbon nanotubes and ruthenium nanoparticles as peroxidase-like nanozyme with supramolecular recognition properties for site-specific anchoring of biotinylated residues," Biosensors and Bioelectronics, vol. 148, p. 111764, 2020.

[22] J. Liu, L. Meng, Z. Fei, P. J. Dyson, L. Zhang, "On the origin of the synergy between the Pt nanoparticles and MnO2 nanosheets in Wonton-like 3D nanozyme oxidase mimics," Biosensors and Bioelectronics, vol. 121, pp. 159–165, 2018.

[23] Q. Chen, S. Li, Y. Liu, X. Zhang, Y. Tang, H. Chai, Y. Huang, "Size-controllable Fe-N/C single-atom nanozyme with exceptional oxidase-like activity for sensitive detection of alkaline phosphatase," Sensors and Actuators B: Chemical, vol. 305, p. 127511, 2020.

[24] J. Xi, C. Zhu, Y. Wang, Q. Zhang, L. Fan, "Mn3O4 microspheres as an oxidase mimic for rapid detection of glutathione," RSC Advances, vol. 9, no. 29, pp. 16509–16514, 2019.

[25] W. Lu, J. Chen, L. Kong, F. Zhu, Z. Feng, J. Zhan, "Oxygen vacancies modulation Mn3O4 nanozyme with enhanced oxidase-mimicking performance for L-cysteine detection," Sensors and Actuators B: Chemical, vol. 333, no. January, p. 129560, 2021.

[26] N. Singh, M. A. Savanur, S. Srivastava, P. D'Silva, G. Mugesh, "A Redox Modulatory Mn3O4 Nanozyme with Multi-Enzyme Activity Provides Efficient Cytoprotection to Human Cells in a Parkinson's Disease Model," Angewandte Chemie International Edition, vol. 56, no. 45, pp. 14267–14271, 2017.

[27] Y. Park, P. K. Gupta, V.-K. Tran, S. E. Son, W. Hur, H. B. Lee, J. Y. Park, S. N. Kim, G. H. Seong, "PVP-stabilized PtRu nanozymes with peroxidase-like activity and its application for colorimetric and fluorometric glucose detection," Colloids Surfaces B Biointerfaces, vol. 204, p. 111783, 2021.

[28] J. Mou, X. Xu, F. Zhang, J. Xia, Z. Wang, "Promoting Nanozyme Cascade Bioplatform by ZIF-Derived N-Doped Porous Carbon Nanosheet-based Protein/Bimetallic Nanoparticles for Tandem Catalysis," ACS Applied Bio Materials, vol. 3, no. 1, pp. 664–672, Jan. 2020.

[29] P. Sengupta, K. Pramanik, P. Datta, P. Sarkar, "Chemically modified carbon nitride-chitin-acetic acid hybrid as a metal-free bifunctional nanozyme cascade of glucose oxidase-peroxidase for 'click off' colorimetric detection of peroxide and glucose," Biosensors and Bioelectronics, vol. 154, no. February, p. 112072, 2020.

[30] H. Wang, J. Zhao, C. Liu, Y. Tong, W. He, "Pt Nanoparticles Confined by Zirconium Metal-Organic Frameworks with Enhanced Enzyme-like Activity for Glucose Detection," ACS Omega, vol. 6, no. 7, pp. 4807–4815, 2021.

[31] X. Han, G. He, Y. He, J. Zhang, X. Zheng, L. Li, C. Zhong, W. Hu, Y. Deng, T.-Y. Ma, "Engineering Catalytic Active Sites on Cobalt Oxide Surface for Enhanced Oxygen Electrocatalysis," Advanced Energy Materials, vol. 8, no. 10, pp. 1–13, 2018.

[32] Z.-J. Chen, Z. Huang, Y.-M. Sun, Z.-L. Xu, J. Liu, "The Most Active Oxidase-Mimicking Mn2O3 Nanozyme for Biosensor Signal Generation," Chemistry – A European Journal, vol. 27, no. 37, pp. 9597–9604, 2021.

[33] T. Mahaseth, A. Kuzminov, "Potentiation of hydrogen peroxide toxicity: From catalase inhibition to stable DNA-iron complexes," Mutation Research, vol. 773, pp. 274–281, 2017.

[34] P. Zhang, D. Sun, A. Cho, S. Weon, S. Lee, J. Lee, J. W. Han, D.-P. Kim, W. Choi, "Modified carbon nitride nanozyme as bifunctional glucose oxidase-peroxidase for metal-free bioinspired cascade photocatalysis," Nature Communications, vol. 10, no. 1, p. 940, 2019.

[35] L. Y. Jin, Y. M. Dong, X. M. Wu, G. X. Cao, G. L. Wang, "Versatile and Amplified Biosensing through Enzymatic Cascade Reaction by Coupling Alkaline Phosphatase in Situ Generation of Photoresponsive Nanozyme," Analytical Chemistry, vol. 87, p. 10429−10436, 2015.

[36] X. Tao, X. Wang, B. Liu, J. Liu, "Conjugation of antibodies and aptamers on nanozymes for developing biosensors," Biosensors and Bioelectronics, vol. 168, p. 112537, 2020.

[37] W. Lu, J. Chen, L. Kong, F. Zhu, Z. Feng, J. Zhan, "Oxygen vacancies modulation Mn3O4 nanozyme with enhanced oxidase-mimicking performance for l-cysteine detection," Sensors and Actuators B: Chemical, vol. 333, p. 129560, 2021.

[38] D. Hassen, S. A. El-Safty, K. Tsuchiya, A. Chatterjee, A. Elmarakbi, M. A. Shenashen, M. Sakai, "Longitudinal Hierarchy Co3O4 Mesocrystals with High-dense Exposure Facets and Anisotropic Interfaces for Direct-Ethanol Fuel Cells," Scientific Reports, vol. 6, no. December 2015, pp. 1–12, 2016.

[39] M. Curti, J. Schneider, D. W. Bahnemann, C. B. Mendive, "Inverse Opal Photonic Crystals as a Strategy to Improve Photocatalysis: Underexplored Questions," The Journal of Physical Chemistry Letters, vol. 6, no. 19, pp. 3903–3910, Oct. 2015.

[40] A. Stein, B. E. Wilson, S. G. Rudisill, "Design and functionality of colloidal-crystal-templated materials—chemical applications of inverse opals," Chemical Society Reviews, vol. 42, no. 7, pp. 2763–2803, 2013.

[41] P. Das, P. Borthakur, P. K. Boruah, M. R. Das, "Peroxidase Mimic Activity of Au–Ag/l-Cys-rGO Nanozyme toward Detection of Cr(VI) Ion in Water: Role of 3,3′,5,5′-Tetramethylbenzidine Adsorption," Journal of Chemical & Engineering Data, vol. 64, no. 11, pp. 4977–4990, Nov. 2019.

[42] B. Çakıroğlu, A. Çiğil-Beyler, A. Ogan, M. V. Kahraman, S. Demir, "Covalent immobilization of acetylcholinesterase on a novel polyacrylic acid-based nanofiber membrane," Engineering in Life Sciences, vol. 18, pp. 254–262, 2018.

[43] L. Cao, P. Wang, L. Chen, Y. Wu, J. Di, "A photoelectrochemical glucose sensor based on gold nanoparticles as a mimic enzyme of glucose oxidase," RSC Advances, vol. 9, no. 27, pp. 15307–15313, 2019.

[44] G.-L. Wang, X. Xu, X. Wu, G. Cao, Y. Dong, Z. Li, "Visible-Light-Stimulated Enzymelike Activity of Graphene Oxide and Its Application for Facile Glucose Sensing," The Journal of Physical Chemistry C, vol. 118, no. 48, pp. 28109–28117, Dec. 2014.

[45] P. Zhang, D. Sun, A. Cho, S. Weon, S. Lee, J. Lee, J. W. Han, D.-P. Kim, W. Choi, "Modified carbon nitride nanozyme as bifunctional glucose oxidase-peroxidase for metal-free bioinspired cascade photocatalysis," Nature Communications, vol. 10, no. 1, p. 940, 2019.

[46] L. Han, H. Zhang, D. Chen, F. Li, "Protein-Directed Metal Oxide Nanoflakes with Tandem Enzyme-Like Characteristics: Colorimetric Glucose Sensing Based on One-Pot Enzyme-Free Cascade Catalysis," Advanced Functional Materials, vol. 28, no. 17, p. 1800018, 2018.

[47] H. Zhang, X. Liang, L. Han, F. Li, "'Non-Naked' Gold with Glucose Oxidase-Like Activity: A Nanozyme for Tandem Catalysis," Small, vol. 14, no. 44, p. 1803256, 2018.

[48] J. Chen, W. Wu, L. Huang, Q. Ma, S. Dong, "Self-Indicative Gold Nanozyme for H2O2 and Glucose Sensing," Chemistry – A European Journal, vol. 25, no. 51, pp. 11940–11944, 2019